2017 International Nuclear Atlantic Conference - INAC 2017
Belo Horizonte, MG, Brazil, October 22-27, 2017
ASSOCIAÇÃO BRASILEIRA DE ENERGIA NUCLEAR – ABEN

Agência Brasileira do ISBN
ISBN 978-85-99141-07-6
9 788599 141076

OPTIMAL TEMPERATURE OF OPERATION OF THE COLD SIDE OF A CLOSED BRAYTON CYCLE FOR SPACE NUCLEAR PROPULSION

Luís F. R. Romano[1], Guilherme B. Ribeiro[1,2]

[1] Instituto Tecnológico de Aeronáutica (ITA)
Pós-Graduação – Ciências e Tecnologias Espaciais
Praça Marechal Eduardo Gomes, 50
12228-900, São José dos Campos, SP
luisromano_91@hotmail.com

[2] Instituto de Estudos Avançados (IEAv)
Departamento de Energia Nuclear
Trevo Coronel Aviador José Alberto Albano do Amarante, 01
12228-001 São José dos Campos, SP
gbribeiro@ieav.cta.br

ABSTRACT

Generating energy in space is a tough challenge, especially because it has to be used efficiently. The optimization of the system's operation has to be though up since the design phase and all the minutiae between conception, production and operation should be carefully evaluated in order to deliver a functioning device that will meet all the mission's goals. This work seeks on further describing the operation of a Closed Brayton Cycle coupled to a nuclear microreactor used to generate energy to power spacecraft's systems, focusing specially on the cold side to evaluate the temperature of operation of the cold heat pipes in order to aid the selection of proper models to numerically describe the heat pipes' and radiator's thermal operation. The cycle is designed to operate with a noble gas mixture of Helium-Xenon with a molecular weight of 40g/mole, selected for its transport properties and low turbomachinery charge, and it is to exchange heat directly with the cold heat pipes' evaporator through convection at the cold heat exchanger. Properties such as size and mass are relevant to be analyzed due space applications requiring a careful development of the equipment in order to fit inside the launcher as well as lowering launch costs. Merit figures comparing both second law energetic efficiency and net energy availability with the device's radiator size are used in order to represent an energetic production density for the apparatus, which is ought to be launched from earth's surface.

1. INTRODUCTION

Given the intrinsic need of energy to execute any kind of work in nature, a thorough design of a power source and its main components is crucial for setting a reliable range of operation and assist on the dimensioning of each component. Usually a viable power source won't provide energy directly in the state as it is needed, therefore said source is commonly associated with an energy conversion system, which is designed specially for a given application and it should be as efficient as possible in order to take advantage of the amount of energy provided by the source while wasting as little as it is thermodynamically permitted.

The goal of this study is to assist on the development of the cold side of an energy conversion system, namely the cold heat pipes and radiators, in order to achieve the best conditions and operating settings. This system is to be coupled to a gas cooled fission microreactor, which is currently under development at the Institute for Advanced Studies (from Portuguese, IEAv) and supported by Brazil's Air Force Command. As defined by Guimarães [1], the

microreactor is part of the project in Advanced Fast Reactor Technology (from Portuguese, TERRA). It operates using fast spectrum neutrons and is intended to generate a few hundred kWe to power spacecraft's needs during missions where the use of conventional means of power generation (i.e. chemical, solar, radioisotopes) cannot be applied or would not suffice.

1.1. Closed Brayton Cycle as Energy Conversion System

Tarlecki et al. [2] evaluate on their study the use of several thermodynamic cycles to be used to convert thermal to electric energy and the Closed Brayton Cycle (CBC) is pointed as the most promising technology for space power system due its high energy efficiency and high power output to radiator area ratio. Being the radiator responsible for the greater portion of the spacecraft's mass, as determined by Juhasz [3] and observed in Figure 1, the evaluation of it's size is crucial to design a system that provides more energy per unit of mass. The CBC operational parameters are discussed in a study developed by Gallo et al. [4] and, later, synthesized by Ribeiro [5] in order to fit the parameters set to represent the operation of the TERRA project.

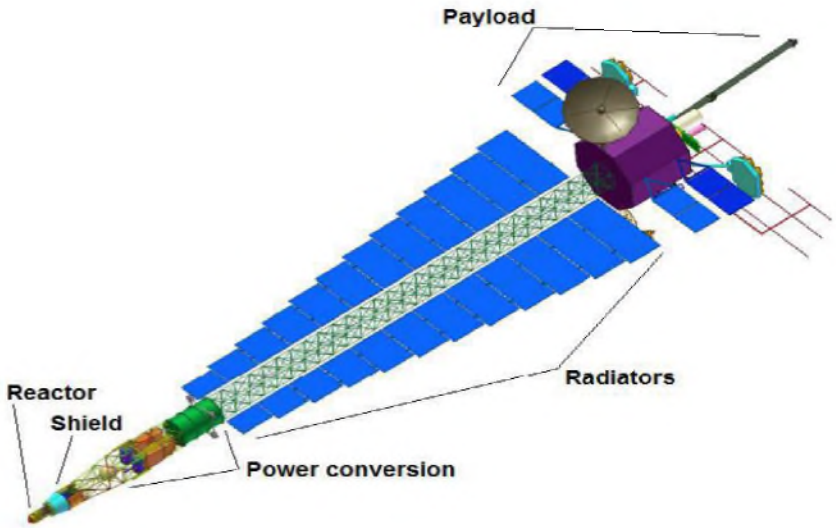

Figure 1: Conceptual nuclear powered spacecraft design with the proposed CBC – Adapted [3].

In order to generate useful energy, the CBC is to be applied between a heat gradient and coupled to an alternator, which will convert the mechanical rotational motion of a turbine into electricity. The reactor's core is considered the heat source – where heat is generated due the fission reactions occurring – and space is considered the heat sink – where heat is rejected to through thermal radiation by the radiators.

Liquid metal heat pipes remove the heat from the core and transfer it at the hot heat exchanger through convection to a mixture of noble gases, used as work fluid of the CBC. The heated mixture expands inside a turbine transforming its energy into mechanical motion, then it proceeds to the hot side of the recuperator where it exchanges heat with fluid that is

leaving the compressor. After leaving the recuperator, the mixture meets the cold heat pipes, which removes the heat of the CBC once again by means of convection, and supply the radiators where it has to be rejected to space. After leaving the cold heat exchanger, the cooled mixture proceeds to the compressor and it is forced through the cold side of the recuperator, where it receives some energy from the hot side before heading to the hot heat exchanger and restarting the cycle all over. The basic arrangement of components that allows the described operation of a CBC can be observed in Figure 2, as well as the representative sections of hot and cold sides of the cycle, containing the reactor and space respectively.

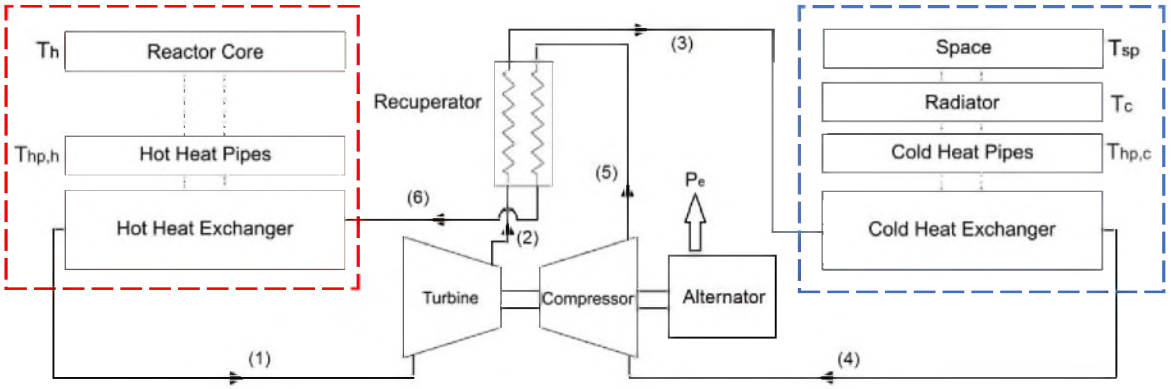

Figure 2: Basic components of proposed CBC with recuperator.

1.2. Cold Side Components of the CBC

Tackling the issues pointed by Juhasz [3], a logical approach on the development of the cold side of the CBC is to correlate the radiators size with its efficiency of removing heat, in order to determine the optimal radiator's size along with its best performance predicted by the thermal models used on the numeric simulation.

In other words, the thermal behavior of the CBC is numerically modeled representing all interfaces where heat is transferred, starting at the hot heat exchanger, considering the operation of the turbine, recuperator, compressor, alternator and all the other components of the cold side, ending when the heat sink is reached. With this representation, the numeric models of the components can be structured and the best parameters to develop a compact conversion cycle set to operate within the reactor's range can be achieved.

To remove the heat from the gas mixture operating inside the cycle the use of heat pipes is of great help, since its employment at the cold heat exchanger region allows the heat to be transferred from the mixture to the radiators with a low temperature drop between its evaporator and condenser sides. Finally, the radiators should be designed taking into account its properties of radiance, form factor and effectiveness, allowing the rejection of the unused generated heat to the space with ease and still being as compact as thermodynamically possible.

Initially, the model of the radiator will be simplified and proper values of its operation are defined as pointed by Ribeiro [5]. This approach seeks to facilitate on the development of the numeric model that will allow the dimensioning of the cold side heat pipes, which need to be

designed to operate within the range that allows the best cycle efficiency to coexist along with the smallest radiator area. The temperature of operation of the cold heat pipes' evaporator ($T_{hp,c}$) is to be determined in order to better select the cold heat pipe material, working fluid and commence its numerical design.

2. METHODOLOGY

Being this study a follow up work and also part of the TERRA project, the model used here to emulate the CBC operation will be considered exactly as described by Ribeiro [5]. The CBC is sectioned and an energy balance is executed on its constituent components. Initially, this approach seeks to determine the amount of energy generated by the thermodynamic conversion cycle given the temperature gradient between the heat source (T_h) and heat sink (T_{sp}) along with core's produced heat (Q_h).

Once the generated (W_{tu}), consumed (W_{co}) and rejected (Q_c) energies are obtained, the next step is to determine the dimensions of the heat exchangers and optimize them observing operational, physical and constructive limitations. Since the hot heat exchanger is directly coupled to the reactor's core, its development should consider the interaction of its constituents with the neutrons generated due the core's operation and how its size affects the nuclear reactions occurrence, for example. As for the cold heat exchanger, properties such as size, overall heat transfer coefficient and coupling are to be evaluated during numeric dimensioning and design.

The considerations regarding the development of the numeric representation of the thermodynamic cycle as well as its cold side are to be discussed on the upcoming sections of this work.

2.1. Modeling the CBC

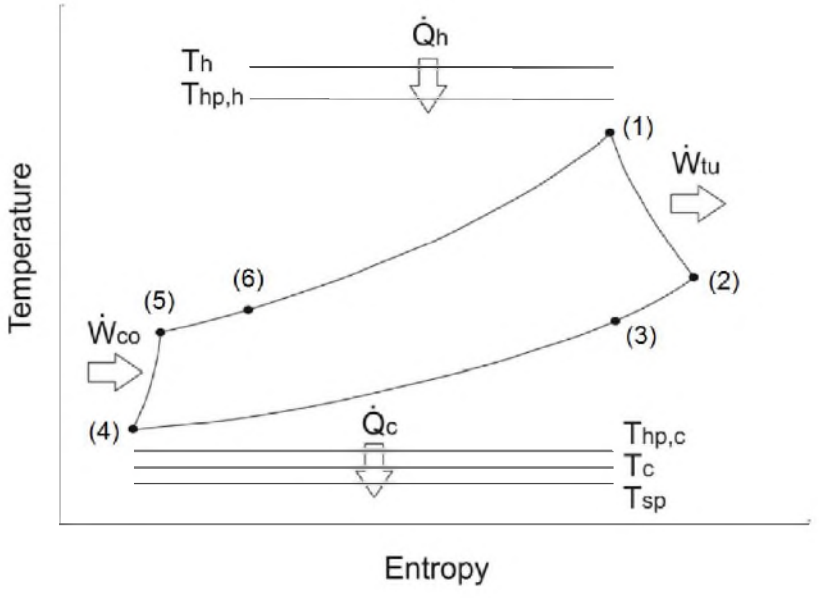

Figure 3: T-s diagram for a CBC with recuperator – Adapted [5].

Along with the previously shown Figure 2, a temperature-entropy diagram for a Brayton cycle with recuperator, presented in Figure 3, can also be used in order to facilitate on the elaboration of the energy balance in each component of the CBC.

As discussed in sections 1.1 and 1.2 of this study, the components responsible to remove heat from the core and the ones that reject it to the radiators are the hot and cold heat pipes, respectively. Both sections can have their operation simplified to represent heat exchangers with constant overall thermal conductance ($UA_{hp,h}$ and $UA_{hp,c}$) and no heat transfer limits. Hence, the temperature drop along each heat pipe is proportional to the heat transfer rate, as seen in equations (1) for the hot and (2) for the cold side of the CBC:

$$\dot{Q}_h = UA_{hp,h}(T_h - T_{hp,h}) \tag{1}$$

$$\dot{Q}_c = UA_{hp,c}(T_{hp,c} - T_c) \tag{2}$$

The core thermal power (Q_h) and its temperature (T_h) are input as fixed values. $T_{hp,h}$ refer to the condenser section of the hot heat pipe, $T_{hp,c}$ to the evaporator section of the cold heat pipe and T_c relates to the condenser side of the cold heat pipe as well as the radiator's temperature of heat rejection – assumed as constant to ease the initial calculations.

To represent the hot and cold heat exchangers, the effectiveness-NTU method was employed as follows:

$$\dot{Q}_h = \dot{m}.c_p(T_{hp,h} - T_6)(1 - e^{\frac{UA_h}{\dot{m}.c_{p,h}}}) \tag{3}$$

$$\dot{Q}_c = \dot{m}.c_p(T_3 - T_{hp,c})(1 - e^{\frac{UA_c}{\dot{m}.c_{p,c}}}) \tag{4}$$

Regarding correlations (3) and (4), $\dot{m}$ refers to the gas mixture mass flow rate, UA_h and UA_c represent the overall thermal conductance of the hot and cold side, whereas the gas constants $c_{p,h}$ and $c_{p,c}$ where obtained based on the temperatures T_6 and T_3, respectively. Still on the heat exchangers, the energy balance on the working fluid is also to be applied on both of them as:

$$\dot{Q}_h = \dot{m}(h_1 - h_6) \tag{5}$$

$$\dot{Q}_c = \dot{m}(h_3 - h_4) \tag{6}$$

The enthalpies at the cold heat exchanger inlet (h_3) and at the compressor outlet (h_5) can be obtained using the correlations for energy balance and effectiveness on the recuperator (ε_r):

$$h_6 - h_5 = h_2 - h_3 \tag{7}$$

$$\varepsilon_r = \frac{(h_2 - h_3)}{(h_2 - h_5)} \tag{8}$$

Representing the operation of the turbine and compressor as polytropic processes and utilizing their efficiencies, η_{tu} and η_{co} respectively, it can be written:

$$\frac{T_1}{T_2} = PR^{\left(\frac{\gamma_{tu}-1}{\gamma_{tu}}\right)\eta_{tu}} \tag{9}$$

$$\frac{T_5}{T_4} = PR^{\left(\frac{\gamma_{co}-1}{\gamma_{co}}\right)\frac{1}{\eta_{co}}} \tag{10}$$

Where γ_{tu} and γ_{co} are the specific heat ratios calculated according to T_1 and T_4, respectively. The pressure ratio (PR), along with the speed ratio (SR), were obtained through an algebraic representation using fourth-order polynomial regression with cross-terms of the performance maps of turbomachinery data for a He-Xe mixture of 40g/mole. As presented by Ribeiro [5], the correlations used to determine PR and SR:

$$\begin{aligned}\dot{m} = {} & A_{tu} + B_{tu}.PR + C_{tu}.PR^2 + D_{tu}.PR^3 + E_{tu}.SR + F_{tu}.SR^2 + G_{tu}.SR^3 \\ & + H_{tu}.PR.SR + I_{tu}.PR^2.SR + J_{tu}.PR.SR^2 + K_{tu}.PR^2.SR^2\end{aligned} \tag{11}$$

$$\begin{aligned}\dot{m} = {} & A_{co} + B_{co}.PR + C_{co}.PR^2 + D_{co}.PR^3 + E_{co}.SR + F_{co}.SR^2 + G_{co}.SR^3 \\ & + H_{co}.PR.SR + I_{co}.PR^2.SR + J_{co}.PR.SR^2 + K_{co}.PR^2.SR^2\end{aligned} \tag{12}$$

η_{tu} and η_{co} are also defined algebraically as

$$\begin{aligned}\eta_{tu} = {} & L_{tu} + M_{tu}.SR + N_{tu}.SR^2 + O_{tu}.SR^3 + P_{tu}.\dot{m} + Q_{tu}.\dot{m}^2 + R_{tu}.\dot{m}^3 \\ & + S_{tu}.SR.\dot{m} + T_{tu}.SR^2.\dot{m} + U_{tu}.SR.\dot{m}^2 + V_{tu}.SR^2.\dot{m}^2\end{aligned} \tag{13}$$

$$\begin{aligned}\eta_{co} = {} & L_{co} + M_{co}.SR + N_{co}.SR^2 + O_{co}.SR^3 + P_{co}.\dot{m} + Q_{co}.\dot{m}^2 + R_{co}.\dot{m}^3 \\ & + S_{co}.SR.\dot{m} + T_{co}.SR^2.\dot{m} + U_{co}.SR.\dot{m}^2 + V_{co}.SR^2.\dot{m}^2\end{aligned} \tag{14}$$

All the coefficients were determined and a precision of no less than 98.8% was achieved for all the described correlations. Single values for PR and SR are obtained after the implementation of the equations.

Finally, it is possible to determine the generated (W_{tu}) and consumed (W_{co}) works by local energy balances at the turbine and compressor, respectively, as well as the rejected heat (Q_c) using a radiative heat transfer correlation for fin-tube geometry:

$$\dot{W}_{tu} = \dot{m}(h_2 - h_1) \tag{15}$$

$$\dot{W}_{co} = \dot{m}(h_5 - h_4) \tag{16}$$

$$\dot{Q}_c = \sigma \varepsilon A_{rad} \eta_f (T_c^4 - T_{sp}^4) \tag{17}$$

The numerical routine presents a solution that is considered valid when the arbitrated mass flow yields a correct match between equations (17) and (4).

Another important value to analyze is the system power efficiency (η_{sys}), which can be represented by the proportion of generated usable work (W_{sys}) when compared to the amount provided by the nuclear core (Q_h), being defined by the following:

$$\eta_{sys} = \frac{\dot{W}_{sys}}{\dot{Q}_h} \tag{18}$$

$$\dot{W}_{sys} = \eta_a (\dot{W}_{tu} - \dot{W}_{co}) \tag{19}$$

Where η_a refers to the alternator's efficiency on converting rotational motion into electricity.

2.2. Merit figures

With the operating CBC described as proposed in the previous section, results for system power efficiency could be generated by changing input values for overall thermal conductance of both cold and hot sides of the cycle. This approach is also used to evaluate the impact of the system's efficiency on the radiators total area needed for radiative heat exchange with the cold heat sink.

To ease the design of the cold heat pipes, it is desirable to determine a temperature range for its operation at the cold heat exchanger. The introduction of merit figures seeks to facilitate on the evaluation of the correlation of the CBC operation and its size under different temperature gradients, due changes on the overall thermal conductance of both sides.

The first merit figure relates the second law's system efficiency ($\eta_{2,sys}$) with the radiator area, being used to determine possible actions to be taken during design in order to minimize the entropy generation on the CBC as a whole while taking into account its direct impact on the radiator's area, hence its total weight. It was determined as:

$$\psi_1 = \frac{100 * \eta_{2,sys}}{A_{rad}} \tag{20}$$

By definition [6], the second law's efficiency represents how distant the evaluated CBC is from its reversible counterpart. This efficiency considers how much energy is lost due irreversibilities on the operation of the cycle, usually sectioned in internal and external irreversibilities, allowing to focus the efforts on optimizing primarily what is responsible for the biggest loss in efficiency.

$$\eta_{2,sys} = \frac{\dot{W}_{sys}}{\dot{W}_{rev}} = 1 - \frac{\dot{W}_{LOST}}{\dot{W}_{rev}} = 1 - \frac{T_{sp} * s_{gen}}{\dot{W}_{rev}} \tag{21}$$

For the W_{LOST}, the model utilizes the relation provided by the second law, which relates the lower temperature on the model (T_{sp}) with the generated entropy (s_{gen}), as presented by equation (21). W_{rev} is given as defined by Carnot for reversible cycles [6] and the definition for the generated entropy (s_{gen}) is given as:

$$\dot{W}_{rev} = \dot{Q}_h \left(1 - \frac{T_{sp}}{T_h} \right) \tag{22}$$

$$s_{gen} = \frac{\dot{Q}_c}{T_{sp}} - \frac{\dot{Q}_h}{T_h} \tag{23}$$

Additionally, a second merit figure is introduced aiming to relate the amount of net mechanical energy available to be converted into electricity with the CBC's radiator area.

$$\psi_2 = \frac{\dot{m}(W_{tu} - W_{co})}{A_{rad}} \tag{24}$$

This variable can then be used to determine a temperature range of operation for the cold heat exchanger which will provide a higher energy availability along with the minimal possible area needed for the function of the CBC.

3. RESULTS AND DISCUSSION

This set of equations were implemented and solved via Newton-Raphson method using Engineering Equation Solver (EES) and the initial goal of the previous study was to determine the minimum radiator area (A_{rad}) in order for the CBC to operate. This was

achieved by Ribeiro [5] and the defined area was around 122.4m², for the predetermined conditions proposed and discussed at his study.

The first analysis was set to observe the behave of the radiator area by varying the value of the temperature of the cold heat pipe's evaporator ($T_{hp,c}$). The minimal and maximal values were determined to fit around the encountered value for $T_{hp,c}$, as it is shown in Figure 4.

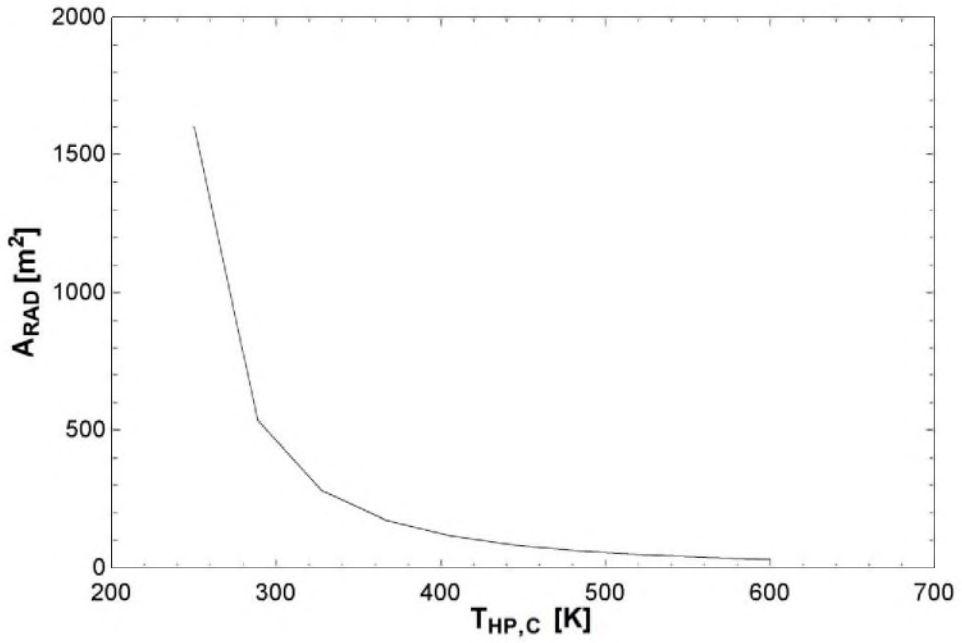

Figure 4: Variation of the radiator's area when compared with the cold heat pipe's evaporator temperature.

It can be noticed that the bigger variation of the area occurs in the interval $250 < T_{hp,c} < 400$, while the region $400 < T_{hp,c} < 600$ presents a lighter slope variation, hence configuring an interesting range of operation to start the design of the cold heat pipes due its lower variation of radiator area.

By evaluating the values for lower $T_{hp,c}$, it can also be observed that the system power efficiency (η_{sys}) will increase due the behavior of a Brayton cycle, which provides more energy when applied between bigger temperature gradients. On the other hand, an increase of radiator area is needed in order to reject all the unused heat the CBC will provide for it's normal operation.

The application of the merit figures discussed in section 2.2 are set to take into account the net energy and radiator size, enabling to analyze how the variation of $T_{hp,c}$ within the desirable range would impact both properties. It was noticed that the behave of both merit figures was similar, peaking around 504K as seen in Figure 5 and Figure 6. Meaning that by optimizing the net energy on the cycle, the second law efficiency would also increase. In other words, the next evaluations can be executed considering only ψ_1 or ψ_2, since they both behave similarly.

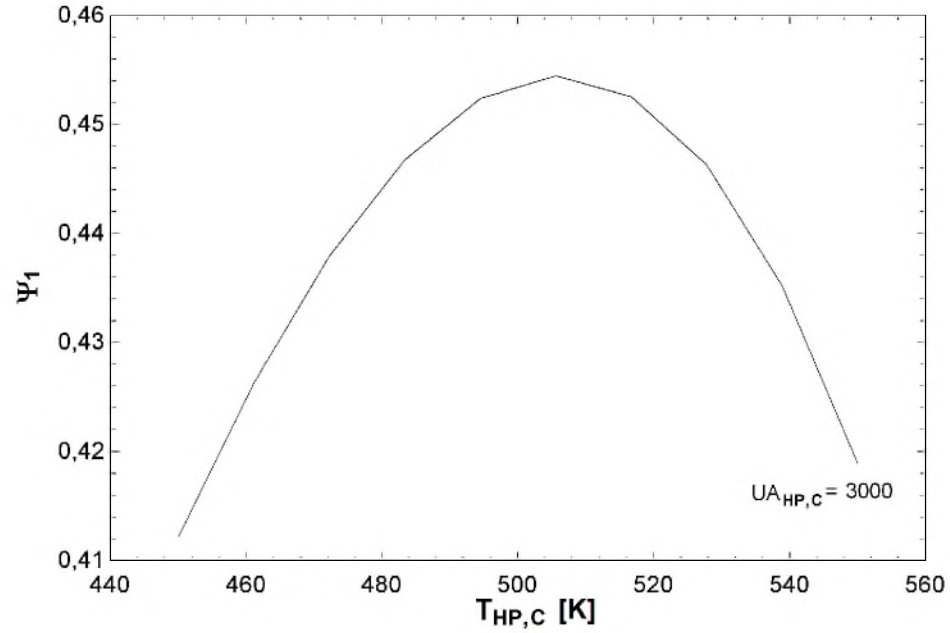

Figure 5: Variation of ψ_1 in comparison with the cold heat pipes' temperature of operation.

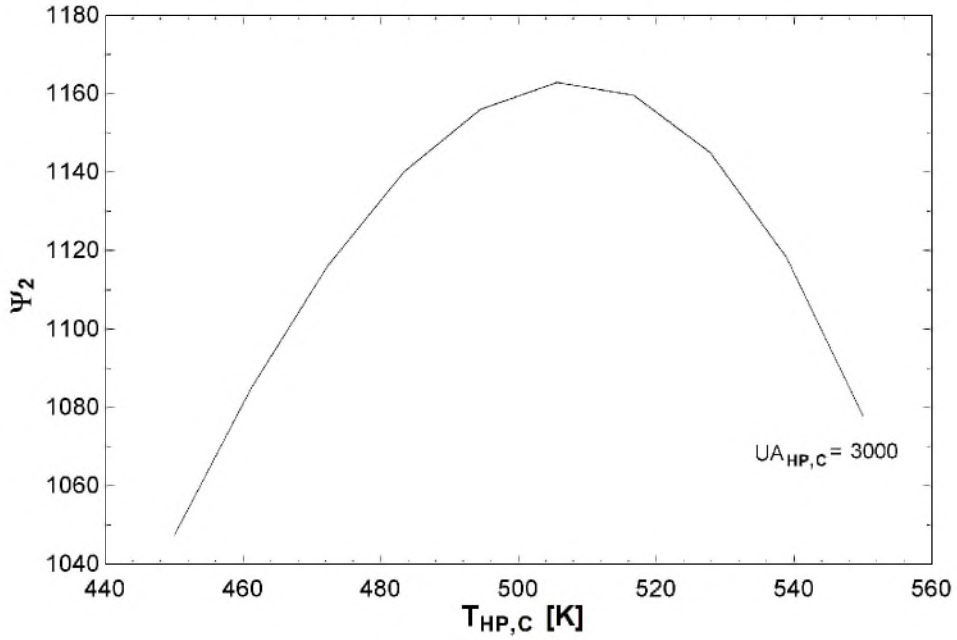

Figure 6: Variation of ψ_2 in comparison with the cold heat pipes' temperature of operation.

It is desirable to maximize ψ_2 value when comparing it to another operating value, such as the overall thermal conductance coefficient of the cold heat exchanger, therefore an analysis on its behave for the determination of initial values for further design on the cold heat pipes is

important. Figure 7 presents the behave of ψ_2 given the variation in the thermal conductance coefficient of the cold side.

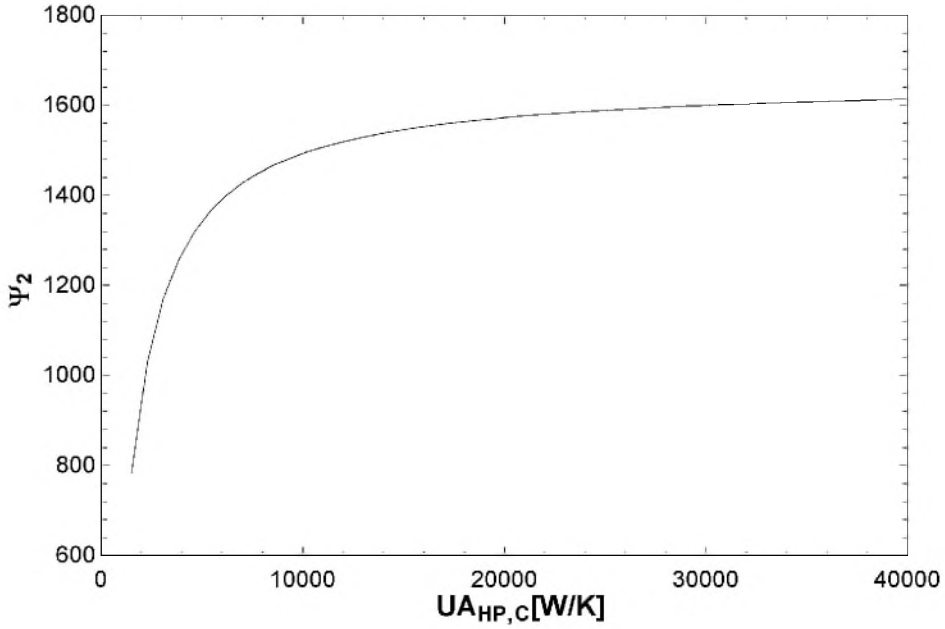

Figure 7: Variation of ψ_2 when compared with the cold heat pipes conductance coefficient.

By observing Figure 7, it can be affirmed that high values of thermal conductance would increase the merit figure as desired, but for space applications compactness is also a fundamental property and should be taken into account.

As it is currently defined on section 2 of this work, the value of $UA_{hp,c}$ can also be linked with the number of heat pipes present for heat extraction from the cycle to the radiators (N_{hp}). This means that a further elaboration on the present model can be achieved by describing the operation of a single heat pipe and calculate its own overall thermal conductance ($UA_{hp,single}$) and comparing with the desirable $UA_{hp,c}$ value, such as:

$$UA_{hp,c} = N_{hp} * UA_{hp,single} \tag{25}$$

Following that reasoning, in order to ease the numeric evaluation and set a more compact system, a smaller variation was determined around the values presented by the operating model solved on EES and the higher and lower limits are as subsequently set as seen in Figure 8. This approach is later to be validated by the comparison with the variation of $T_{hp,c}$ and its effect on ψ_2. If the temperature of operation is function of the $UA_{hp,c}$ the peak values for the temperature will vary for each curve, requiring to reevaluate the best temperature of operation every time $UA_{hp,single}$ or N_{hp} changes.

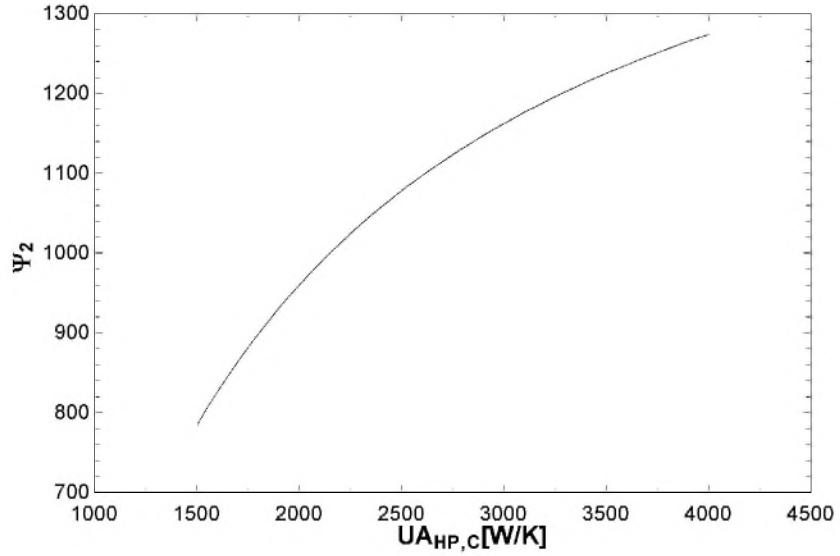

Figure 8: Analyzed range of cold heat pipes conductance coefficient.

An increase in $UA_{hp,c}$ will directly impact the overall mass of the CBC by increasing the number of heat pipes or augmenting its overall thermal conductance, as presented previously by correlation (25). Figure 9 represents the variation of temperature and its effect on ψ_2 for the $UA_{hp,c}$ determined as presented in Figure 8. From the analysis, it can be concluded that despite the variation of $UA_{hp,c}$, being it caused by the variation in $UA_{hp,single}$ or N_{hp}, all peaks will be around 504K, setting an optimal range of temperature around that value for a heat pipe array of any size.

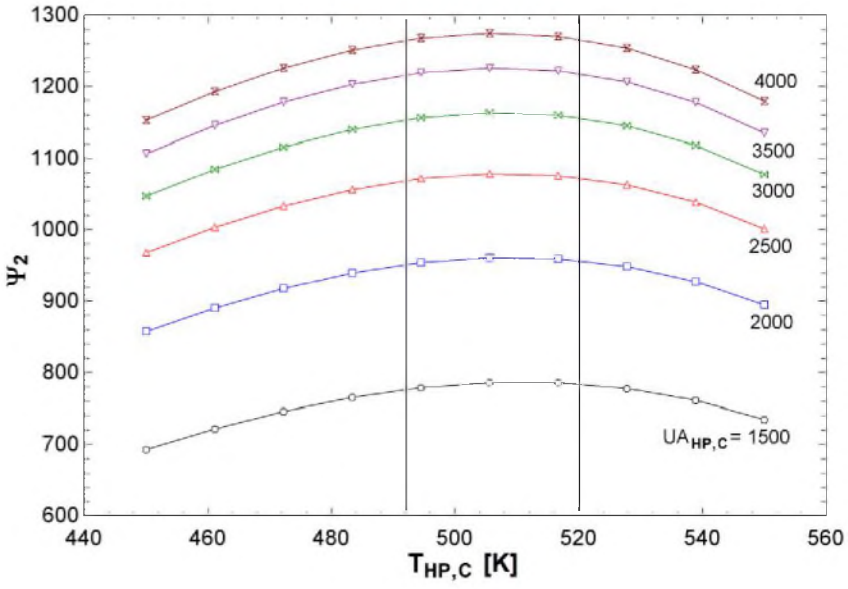

Figure 9: Optimal temperature range of operation of the CBC's cold heat pipes.

The optimal range for the cold heat pipes to operate can also be determined by maximizing the value of ψ_2 when compared to the values of thermal conductance, presented in Figure 10

for various values of $T_{hp,sink}$, considering a temperature range within the section that presented lower values for A_{rad} on Figure 4, as commented before.

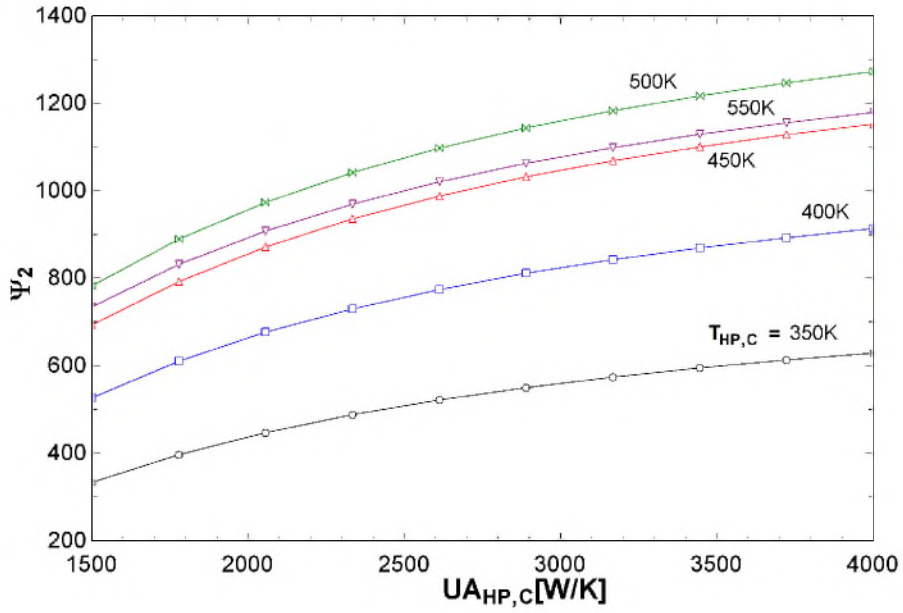

Figure 10: Optimal temperature range of operation of the CBC's cold heat pipes.

The curves show an increase in values for ψ_2 when $350 < T_{hp,sink} < 500$ and a decrease after this value, therefore the previous conclusions on the analysis of Figure 9 are considered correct and defined as the optimal temperature range to start the development of the cold side heat pipes.

By determining the optimal $T_{hp,sink}$ as ranging around 500K, previous concepts on the TERRA project regarding copper-water porous wicked heat pipes on the cold side can be discarded given their maximal operating temperature being lower than 425K, as pointed by Anderson [7]. A possible option for the cold side heat pipes could be titanium-water grooved heat pipes, which fits the temperature range and presents a smaller wall configuration needed to withhold the saturation pressure of the fluid inside while operating, while also being able to be manufactured.

4. CONCLUSIONS

Given the operation of the cycle determined by the described numeric representation, for various values of thermal conductance on the cold heat exchanger, the temperature range determined as optimal for maximizing the CBC efficiency while minimizing the radiator area is set as ranging from 490K up to 520K. Namely, this is determined on the model as the operating temperature for the cold heat pipe's evaporator, which has the function of transferring heat from the work fluid to the space radiators.

The determination of an operating temperature range is an important factor for the heat pipe design given the analysis needed to evaluate its structural and physical properties during its

conception. A relevant design characteristic for the heat pipes is the wall configuration and thickness needed to withhold the saturation pressure of the work fluid inside while operating. By deciding to operate with titanium instead of copper, there is also the need to change the heat pipe modeling, since the first usually is represented operating with the use grooves and fins to pump the fluid from the condenser to the evaporator, while the second applies a porous mesh for this purpose. This means that the numeric representation for a porous wicked differs from the grooved, thus the evaluation for the optimal temperature of operation provided here also helps on the definition of the heat pipe's material and heat transfer description.

Looking ahead on easing future works, the determined material also leaded to machining limitants, being this the reason why this study decided on changing to a grooved wick for future model implementation. If decided on keeping the models for porous wick, it would be necessary to consider different material and methods to elaborate and machine the heat pipe.

Also, as presented by equation (25), the $UA_{hp,c}$ is linked to the number of cold heat pipes and this description is to be used in future works in order to evaluate the best array of heat pipes. Furthermore, the evaluation on total heat exchanger mass, for both hot and cold sides, can be elaborated only after considering the results for the cold side size after coupling to this work models for the heat pipes and radiator, representing their operation.

ACKNOWLEDGMENTS

This study is part of TERRA program, sponsored by the Ministry of Defense (V01010109) and Air Force Command. The help of all coworkers at IEAv is highly appreciated and was an important part on the development of this work.

REFERENCES

1. L. N. F. Guimarães *et al.*, "Basic Research and Development Effort to Design a Micro Nuclear Power Plant for Brazilian Space Application," *Nucl. Emerg. Technol. Sp. 2011*, p. 9, (2011).
2. J. Tarlecki, N. Lior, and N. Zhang, "Analysis of thermal cycles and working fluids for power generation in space," *Energy Convers. Manag.*, **vol. 48**, no. 11, pp. 2864–2878, (2007).
3. A. Juhasz, "Heat Transfer Analysis of a Closed Brayton Cycle Space Radiator," *5th Int. Energy Convers. Eng. Conf. Exhib.*, no. June, pp. 25–27, (2007).
4. B. M. Gallo and M. S. El-Genk, "Brayton rotating units for space reactor power systems," *Energy Convers. Manag.*, **vol. 50**, no. 9, pp. 2210–2232, (2009).
5. G. B. Ribeiro, F. A. Braz Filho, and L. N. F. Guimarães, "Thermodynamic analysis and optimization of a Closed Regenerative Brayton Cycle for nuclear space power systems," *Appl. Therm. Eng.*, **vol. 90**, pp. 250–257, (2015).
6. A. Bejan, *Advanced Engineering Thermodynamics*, John Wiley & Sons, Hoboken USA, (2006).
7. W. Anderson, P. Dussinger, R. Bonner, and D. Sarraf, "High Temperature Titanium/Water and Monel/Water Heat Pipes," *4th Int. Energy Convers. Eng. Conf. Exhib.*, no. June, pp. 26–29, (2006).